A soft-contact model for computing safety margins in human prehension

Tarkeshwar Singh[1], Satyajit Ambike[2]

[1]*College of Health Professionals, Medical University of South Carolina, Charleston, SC-29425*
[2]*Department of Kinesiology, Purdue University, West Lafayette, IN-47907*

Keywords: soft-contact, safety margins, friction, grasp planning, prehension.

POSTPRINT *(To appear in Human Movement Science)*

Final publication is available at:

Address for Correspondence:
Tarkeshwar Singh
Department of Health Sciences and Research
Medical University of South Carolina
77 President Street
Charleston, SC-29425
Email: singht@musc.edu
Phone: 843-792-7685

Highlights

- A novel soft-contact based safety margin model is proposed for studying human prehension.
- The model provides a mechanics based measure for computing safety margins.
- The model also quantifies how free moments applied by the digits contribute to grasp stability.

Abstract

The soft human digit tip forms contact with grasped objects over a finite area and applies a moment about an axis normal to the area. These moments are important for ensuring stability during precision grasping. However, the contribution of these moments to grasp stability is rarely investigated in prehension studies. The more popular hard-contact model assumes that the digits exert a force vector but no free moment on the grasped object. Many sensorimotor studies use this model and show that humans estimate friction coefficients to scale the normal force to grasp objects stably, i.e. the smoother the surface, the tighter the grasp. The difference between the applied normal force and the minimal normal force needed to prevent slipping is called safety margin and this index is widely used as a measure of grasp planning. Here we define and quantify safety margin using a more realistic contact model that allows digits to apply both forces and moments. Specifically, we adapt a soft-contact model from robotics and demonstrate that the safety margin thus computed is a more accurate and robust index of grasp planning than its hard-contact variant. Previously, we have used the soft-contact model to propose two indices of grasp planning that show how humans account for the shape and inertial properties of an object. A soft-contact based safety margin offers complementary insights by quantifying how humans may account for surface properties of the object and skin tissue during grasp planning and execution.

1 Introduction

In the sensorimotor control literature, safety margin, the normalized difference between the applied grip force and the minimal grip force to prevent slipping (Hermsdörfer, Hagl, Nowak, & Marquardt, 2003; Westling & Johansson, 1984), is frequently used to quantify grasp planning. The minimal grip force is prescribed by the object's weight and the friction coefficient between the glabrous skin of the hand and the grasped object. Humans scale grip forces by estimating the friction coefficient between the digits and the grasped object: the smoother the surface, the larger the applied grip force (reviewed in Flanagan & Johansson, 2010).

This analytical framework is based on the hard-contact model which assumes that digits can apply a three-dimensional force vector but no free moment to the object. The hard-contact model presumes that a grasped object will not slip from the fingers as long as the force vector at each digit-object contact is in the interior of a friction cone (defined in the 3D space of contact forces). However, this model does not capture the richness of the human prehension repertoire (Singh & Ambike, 2015). The dynamic interactions between the human digits and grasped objects are more realistically modeled as soft contacts in which the digits apply a three-dimensional force to the object and a free moment about the normal to the contact surface. Here, we propose a soft contact based safety margin and demonstrate how it can be used to quantify grasp planning and stability.

In his pioneering work, Heinrich Hertz described the geometry and stress distribution of two elastic bodies in contact and exerting only a normal force on each other (Hertz, 1882). His model was further developed and validated for non-linear material properties, including human fingers (Kao & Cutkosky, 1992; Li & Kao, 2001; Xydas & Kao, 1999). These authors added the Coulomb friction model and allowed a 3D force vector and a moment about the contact-area normal to the applied contact site. These contact characteristics, which define a soft contact (Murray, Li, & Sastry, 1994), constitute a realistic model to study human digit-object interactions. It has been widely used in robotics (Yoshikawa, 2010), but to the best of our knowledge has only been introduced in a few studies of human prehension (Kinoshita, Bäckström, Flanagan, & Johansson, 1997; Shim, Latash, & Zatsiorsky, 2005; Singh & Ambike, 2015). Kinoshita et al.'s model of safety margin for soft contacts is data driven and does not provide a mechanistic framework to quantify grasp planning. Furthermore, their model is only applicable to a specific experimental design where the applied external loads are assumed to be in one plane, and consequently, their results are not generalizable to an object grasped in an arbitrary orientation.

Here, we review the hard- and soft-contact models in Section 2. We propose a soft contact based safety margin as a complementary measure of grasp mechanics that reflects how humans execute grasps by accounting for surface friction (Adams, et al., 2013; Cadoret & Smith, 1996) and local physiological changes. Since our model is based on mechanics, it is not constrained by the limitations of Kinoshita et al.'s model (Kinoshita, et al., 1997) and can be used to study grasps in any arbitrary configuration.

We also propose a mathematical framework for the implementation of a soft contact based safety margin for human prehension. In Section 3, we reinterpret data from a previous study (Singh, Zatsiorsky, & Latash, 2013) to illustrate the utility of the proposed metric. Finally, in Section 4, we discuss our findings and conclude by discussing the potential applications and benefits of a soft-contact model.

2 Methods

2.1 Contact models

2.1.1 A hard-contact friction model and safety margin

For hard-contact models, the friction cone determines the ratio of tangential to normal forces that can be exerted on the object without slipping (Fig. 1A). The cone surface is a boundary, and the contact force vector must lie within this boundary for a stable contact to occur (i.e., contact without slip). If Coulomb's law of friction is employed, the Friction Limit Surface (FLS) is a cone given by:

$$\frac{(x_F)^2+(y_F)^2}{(\mu_s)^2} = (z_F)^2 \quad (1)$$

where x_F, y_F and z_F are variables for the two orthogonal tangential forces and the normal force, respectively (see Fig. 1A). We then define the applied force vector, $\mathbf{W_{applied}} = [F^X, F^Y, F^Z]$. That is, we view the subject's actual finger forces F^X, F^Y, and F^Z as specific values plotted along the x_F, y_F and z_F axes, respectively. The vector $\mathbf{W_{applied}}$ is called the slip vector, consistent with the robotics literature (Kao & Cutkosky, 1992). The key idea

is that the slip vector is constrained to lie within the FLS to prevent slipping. The cone surface (FLS) in Figure 1A represents the condition in which the normal force F^Z is exactly sufficient to generate sufficient tangential force to balance the inertial load imposed by the object. The slip vector in Figure 1A is a loading at a finger-object contact. The vector is in the interior of the FLS, so there is no slip. Furthermore, the tangential force components of the vector are determined by the friction coefficient and the object-induced inertial loads. However, the normal force is applied by the subject, and it determines the location of the slip vector relative to the FLS. In typical static grasping experiments that implement planar analyses, the tangential component of the applied force vector ($\|F^{X,Y}\| = \sqrt{(F^x)^2 + (F^y)^2}$), is determined by the weight of the object alone, and the other tangential component orthogonal to the weight vector is 0 (i.e. either F^X or F^Y =0). However, $F^{X,Y}$ for a grasped glass that is being transported from a table to the mouth for a sip would have two non-zero tangential force components.

This implies that, in planar grasps, the minimum normal force required to avoid slip is $F^Z_{min} = \|F^{X,Y}\|/\mu_S$. Then, Safety Margin (SM) for a grasp modeled using hard contact is defined as the proportion of the applied normal force above the threshold for slippage (Aoki, Niu, Latash, & Zatsiorsky, 2006; Jenmalm, Goodwin, & Johansson, 1998):

$$SM_{hard} = \left[\|F^Z\| - \|F^Z_{min}\|\right] \Big/ \|F^Z\| \qquad (2)$$

For human prehension, many studies have shown that μ_s decreases with an increase in the applied normal force (Savescu, Latash, & Zatsiorsky, 2008; Seo, Armstrong, & Drinkaus, 2009; Tomlinson, Lewis, & Carré, 2007). We use the following non-linear relationship that was derived from the data presented in the study by Savescu and colleagues:

$$\mu_s = 1.44(\|F^Z\|)^{-0.293} \qquad (3)$$

2.1.2 A soft-contact model and safety margin

In soft-contact models, a digit exerts a four-dimensional wrench (3 orthogonal forces and a moment about a normal to the contact area). For such wrenches, the Friction Limit Surface (FLS) given by a friction cone in the force space (for a hard contact model) is replaced by a FLS in a space defined by the tangential forces and the free moment (Fig. 1B). Specifically, the FLS is an ellipsoid defined as:

$$\frac{(x_F)^2+(y_F)^2}{(\mu_s F^Z)^2} + \frac{(z_\tau)^2}{(T^Z_{max})^2} = 1 \quad (4)$$

where x_F, y_F and z_τ are variables for the tangential forces and free moment, respectively (Fig. 1B). F^Z is the applied normal force and T^Z_{max} is the magnitude of the maximum moment that can be applied without slip. It is approximated as:

$$T^Z_{max} = 0.59 a \mu_s F^Z \quad (5a)$$

$$a = C(F^Z)^\gamma \quad (5b)$$

where ‘a’ is the radius of the contact area as a function of F^Z , C ≈ 2.0 and $0.11 \leq \gamma \leq 0.17$ for human fingers (Xydas & Kao, 1999). ‘C’ is a constant that depends on the size and curvature of the tip as well as the material properties of the grasped object. Thus, the applied normal force F^Z determines the FLS for a given finger-object pair. Increasing F^Z expands the ellipsoid and increases the enclosed volume.

We then define the slip vector, $\mathbf{W_{applied}} = [F^X, F^Y, T^Z]$, applied by the participant and in the soft-contact model, it comprises of the tangential forces and free moment (Kao & Cutkosky, 1992). The applied slip vector, $\mathbf{W_{applied}}$, must lie within the FLS determined by the normal force to prevent slipping. We then define the safety margin as the signed shortest distance between $\mathbf{W_{applied}}$ and the FLS normalized by the magnitude of the normal force. To compute this safety margin, the shortest distance between the tip of $\mathbf{W_{applied}}$ and the nearest point on the FLS, $\mathbf{W_{nearest}}$ is computed using Lagrange’s multipliers (Eq. 6a). We denote $\mu_s F^Z$ and T^Z_{max} from Eq. 4 as ‘m’ and ‘n’, respectively, and substitute the partial derivatives of the Lagrangian L with respect to x_F, y_F and z_τ to get Eq. 6b.

$$L = \left\{\left(x_F - F^X\right)^2 + \left(y_F - F^Y\right)^2 + \left(z_\tau - T^Z\right)^2\right\} + \lambda\left[\frac{(x_F)^2 + (y_F)^2}{(m)^2} + \frac{(z_\tau)^2}{(n)^2} - 1\right] \quad (6a)$$

$$\frac{\partial L}{\partial \lambda} = \frac{\left(mF^X\right)^2}{(\lambda + m^2)^2} + \frac{\left(mF^Y\right)^2}{(\lambda + m^2)^2} + \frac{\left(nT^Z\right)^2}{(\lambda + n^2)^2} - 1 = 0 \quad (6b)$$

Eq. 6b yields a 4th order polynomial in λ and is solved using a root-finding algorithm. A real value of λ (= λ^*) that minimizes the distance is selected, and then the components of $\mathbf{W}_{\mathbf{nearest}}$ are given by

$$x_{F,nearest} = \frac{m^2 \times F^X}{\lambda_* + m^2};\ y_{F,nearest} = \frac{m^2 \times F^Y}{\lambda_* + m^2};\ z_{\tau,nearest} = \frac{n^2 \times T^Z}{\lambda_* + n^2} \quad (7)$$

Safety margin for the soft contact is then computed as

$$SM_{soft} = \text{sign}\left(\|\mathbf{W}_{\mathbf{nearest}}\| - \|\mathbf{W}_{\mathbf{applied}}\|\right) \times \frac{\left\|\mathbf{W}_{\mathbf{nearest}} - \mathbf{W}_{\mathbf{applied}}\right\|}{\|F^Z\|} \quad (8)$$

Note that $SM_{soft} > 0$ when $\mathbf{W}_{\mathbf{applied}}$ is within the FLS, and is equal to or less than zero when $\mathbf{W}_{\mathbf{applied}}$ touches or intersects the FLS. The latter case is useful for investigating the safety margin dynamics in grasp-and-lift behaviors.

Figure 2 shows the safety margins computed using simulations for the hard-contact and soft-contact models (Eqs. 2 and 8, respectively) as functions of normal force and free moment. In Figure 2A, the free moment is held constant when computing SM_{soft}. The two contact models yield different safety margins, and SM_{soft} is also influenced by the applied/required free moment. Panel B shows that for a constant normal force, SM_{soft} decreases as the applied/required free moment increases in magnitude.

2.2 Application to experimental data

Here, we reinterpret data from a previous study (Singh, et al., 2013) by applying the new metric introduced in the previous sections. The goal of the original study was to

investigate the effects of exercise-induced fatigue on grasp mechanics. The objective here is to use the data from that study to illustrate how SM_{soft} can offer novel insights into the biomechanics and the motor control of prehensile behavior.

2.2.1 Participants

Eight participants (four males) volunteered to participate in the study. Their average age, height and weight was 28.3 ± 4.9 yrs, 1.73 ± 0.10 m, 67.9 ± 9.02 kg, respectively. All the participants were free of known neurological or muscular disorders and were right hand dominant. They gave informed consent based on the procedures approved by the Office for Research Protection of the Pennsylvania State University.

2.2.2 Experimental setup

The details of the experimental paradigm are provided in previous publications (Singh, et al., 2013; Singh, Zatsiorsky, & Latash, 2014). Briefly, five six-component sensors (model Nano 17-R; ATI, Apex, NC, USA) were used to measure the forces and moments produced by the individual digits. Sandpaper (100 grit) was placed on the contact surface of each sensor to provide friction. These sensors were attached to an aluminum handle (see Fig. 3) and the total weight of the setup was ~8.96 N.

2.2.3 Fatigue setup

The fatiguing exercises were performed on the apparatus shown in the inset of Figure 3. A one-dimensional strain gauge sensor recorded the force output of the thumb.

Feedback of the force exerted by the thumb was provided to the participants on a laptop placed 80 cm in front of the participant. This setup was expected to induce fatigue in the thumb flexors, namely, opponens pollicis, flexor pollicis brevis, and flexor pollicis longus (FPL), and the first dorsal interosseous (Luu, Day, Cole, & Fitzpatrick, 2011).

2.2.4 Experimental protocol

Participants lifted the handle with their right hand (dominant) and maintained it parallel to the horizontal for 5 seconds (one trial) and repeated 20 trials each in three blocked conditions; NEUT (no external torque), PR (pronation torque) and SUP (supination torque). The external torques were necessary to elicit strong tangential forces and moments (see Fig. 3). Prior to starting the experiment, participants performed practice trials for each torque condition. At the conclusion of the 20 control trials for each torque condition, the participants performed the fatiguing exercise for one minute. Then they repeated 20 grasping trials (in each condition) with a 20 second fatiguing exercise every 5 trials to prevent recovery. The order of the torque conditions was randomized across participants.

2.3 Statistics

We computed safety margins based on hard-contact as well as soft-contact models only for the fatigued digit, the thumb, because initial slip was most likely to occur there.
The study had a two-factor design with ‘fatigue’ as the first factor (before and during fatigue as levels) and ‘torque’ as the second factor (NEUT, PR and SUP as levels). A two-way repeated measures ANOVA was first performed to test the main and

interaction effects of the two factors. The level of significance was chosen at α=0.05. Our analysis revealed no main or interaction effects involving 'torque' for either SM_{Hard} or $SM_{Soft.}$ Therefore, this factor was eliminated from further analysis. Paired t-tests were then performed for the before fatigue (control) and during fatigue conditions by averaging the data across the three torque conditions.

3 Results

Figure 4A shows the changes in the tangential forces (F^X and F^Y), normal force (F^Z) and moment (T^Z) during fatigue for the fatigued digit, i.e., the thumb. The normal force decreased, but all other wrench components increased in magnitude during fatigue. Paired t-tests confirmed significant differences between the two conditions for all four variables. For the soft-contact model, on the one hand, the decrease in normal force reduces the volume encompassed by FLS and, on the other hand, the increase in the tangential force components and free moment increase the magnitude of the applied slip vector (Fig. 4B). Figure 4B shows that the tip of the slip vector gets closer to the FLS during fatigue, thus, rendering the grasp less stable. The differences in the relative magnitudes of the slip vectors can be seen more clearly in Figure 4C.

Figures 5A and 5B show the group differences in safety margins (SM_{Hard} and SM_{Soft}) for the before and during fatigue conditions for the thumb. Safety margins decreased for both the models ($p < 0.01$) but the drop was larger for $\mathrm{SM}_{\mathrm{Hard}}$ than $\mathrm{SM}_{\mathrm{soft}}$ by about 25%. Furthermore, the coefficients of variation of safety margins were identical for the two contact models (0.48 and 0.46 for $\mathrm{SM}_{\mathrm{Hard}}$ and $\mathrm{SM}_{\mathrm{soft}}$, respectively). Thus, the results

from the two models are qualitatively identical. However, since the $\mathrm{SM}_{\mathrm{soft}}$ values are computed from a more physically accurate model, they provide a more accurate representation of grasp stability and are likely to be more reliable in predicting failure, i.e., slip.

4 Discussion

4.1 Relation between the safety margins using the hard- and soft-contact models

Safety margins have been used to investigate deficits in sensorimotor control of prehension due to cerebellar lesions (Rost, Nowak, Timmann, & Hermsdörfer, 2005), stroke (Nowak, 2008), aging (Cole, Rotella, & Harper, 1999) and applied anesthesia (Johansson & Westling, 1984). Typically, studies compute safety margins using the hard-contact model to measure the difference between the applied grip force (normal) and minimal grip force. The minimal grip force is determined by the friction coefficient and the object's kinematics. Thus, safety margins for hard-contact models are mainly driven by changes in normal forces and the object's movement.

The notion of the safety margin is linked to that of the friction limit surface (FLS). The FLS exists in a space defined by the dynamic variables (forces and moments) that can exist at the contact between two objects. It separates the space into two distinct regions. In the stable region (the interior of the FLS), there is no slip between the contacting bodies, i.e., the forces and moments acting at the contact are not sufficient to create relative motion between the bodies. Conversely, the complementary region

(exterior to the FLS) is unstable, meaning that slip between the contacting bodies exist. The FLS used for the hard- and soft-contact models (Equations 1 and 4, respectively), can be obtained from a single equation:

$$\frac{(x_F)^2+(y_F)^2}{(\mu_s z_F)^2} + \frac{(z_\tau)^2}{\left(T^Z_{max}\right)^2} = 1 \quad (9)$$

Note that the denominator of the first term in the left-hand side of Equation 9 uses the variable z_F rather than the applied normal force F^z (as in Equation 4). Equation 9 is a single, non-linear constraint on four variables x_F, y_F, z_F and z_τ, and it represents a manifold in that four-dimensional space. The hard-contact model ignores z_τ ($z_\tau = 0$), yielding Equation 2. In other words, the FLS for hard contact (the cone in Figure 1A) is the intersection of the 4-dimensional manifold represented by Equation 9, and the plane, z_τ =0. Equation 4 is the intersection of the above manifold with the plane $z_F = F^Z$. The advantage of using Equation 4 rather than Equation 9 for the soft-contact model is that the intersection set can be visualized and depicted as a 3-dimensional object (the ellipsoid in Figure 1B). Therefore, it is clear that the FLS for the soft-contact model reduces to the FLS for the hard-contact model in the special case when there is no external torque acting at the contact.

However, SM_{soft} does not become identical to SM_{hard} for most physically meaningful loadings between contacting surfaces. Although ignoring the free moment implies that the FLS for the hard and soft-contact models are identical (the cone in Figure 1A), this does not lead to the same SM for hard and soft-contact models (Fig. 2A). This is because SM_{hard} is the ratio of the excess normal force applied by the digit to the

minimum normal force required to avoid slip (i.e., a ratio along the z_F coordinate), whereas, SM_{soft} is the minimum distance between $\mathbf{W_{applied}}$ and the FLS divided by F^Z. However, SM_{hard} and SM_{soft} approach each other when two conditions are met: (1) there is no free moment, and (2) the normal force is very small (Fig. 2A). These conditions may be encountered during precision manipulation, and in those specific cases, both safety margins will yield similar results. However, for most activities of daily living and most experimental paradigms, SM_{hard} and SM_{soft} are not expected to be similar.

It should also be noted that in this report we are using the definition of SM_{hard} (Eq. 2) that has been used previously in the sensorimotor control literature (Aoki, et al., 2006; Jenmalm, et al., 1998). Indeed, SM_{hard} can be defined analogously to SM_{soft} by computing how close the slip vector ($\mathbf{W_{applied}} = [F^X, F^Y, F^Z]$, for the hard-contact model) is to the friction cone surface:

$$SM_{hard} = \tan^{-1}(\mu_s) - \tan^{-1}\left(\frac{\|F^{X,Y}\|}{\|F^Z\|}\right) \qquad (10)$$

where, μ_s is the friction coefficient. For the sandpaper affixed to the sensors in the current study, μ_s can be computed using Equation 3. For other contact surfaces, it should be experimentally determined. It should also be noted that the SM_{hard} defined in Eq. 10 is an angular measure and not a measure of distance like SM_{soft} in Eq. 8. Therefore, Equation 10 is analogous to Eq. 8 but cannot be derived from it. For the purpose of experimental validation (see next section), we use the traditional definition of SM_{hard} from Equation 2.

4.2 Experimental validation.

To illustrate the utility of the new metric SM_{soft}, we utilized the data from a previous study (Singh, et al., 2013) that involved fatiguing the thumb. The safety margins before and during fatigue were computed using both SM_{hard} and SM_{soft}. The safety margin based on the hard-contact model (Eq. 2) reflects fatigue induced declines in the applied normal forces only (Fig. 4A & 5A). It does not account for changes in the free moments applied by the digits. However, free moment plays a key role in stabilizing precision grasps (Singh & Ambike, 2015), especially if the grasped object is asymmetric and applies a net moment on the hand (Shim, et al., 2005). Our experimental paradigm was designed to elicit free moments by the digits, and we expected the moments to also change during fatigue. The soft-contact based safety margin, SM_{soft}, allows us to account for the free moments, and we show that during fatigue, the volume of the FLS decreased and the magnitude of the applied slip vector ($\|\mathbf{W}_{\mathbf{applied}}\|$) increased. Consequently, $\mathbf{W}_{\mathbf{applied}}$ was closer to the boundary of FLS (Fig. 4B,4C), the safety margin was lower, and the grasp was less stable. Indeed, during fatigue there were larger kinematic fluctuations in the grasped handle suggesting that there could be small slips at the digit-object interface. During fatigue, the standard deviation of the handle orientation about its mean increased by about ~150-200% during a trial along all three cardinal axes ($p<0.001$). Similarly, the standard deviation of the handle position about the mean location increased by ~130-200% during fatigue ($p<0.01$) along all three axes. The increased $\|\mathbf{W}_{\mathbf{applied}}\|$ during fatigue in the soft-contact model (due to increases in F^X, F^Y, T^Z, see Fig. 4A), implies greater effort, and yet, this effort results in a lower

safety margin (smaller FLS due to decrease in F^Z during fatigue). This reduced stability at the fatigued digit may result from the different mechanical effects of altering motor-unit recruitment during fatigue (Carpentier, Duchateau, & Hainaut, 2001; Xia & Law, 2008).

Previously, using the soft-contact model, we computed grasp caliber and grasp intensity, that measure how the inertial properties of the object (shape, size, weight) are accounted for during grasp planning for the purpose of digit placement and wrench magnitude selection, respectively (Singh & Ambike, 2015). However, neither index addressed the friction requirements for grasp stability, and, perhaps unsurprisingly, one of the indices, grasp intensity, was insensitive to exercise-induced fatigue. The null results suggested that exercise-induced fatigue alters digit placement on the object, perhaps to minimize discomfort, but grasp intensity, which reflects the overall neural drive to all digits is relatively unaffected. In contrast, safety margin is digit-specific (Kinoshita, et al., 1997), it was computed for the digit where slip was most likely to occur, and therefore, it was sensitive to fatigue (Fig. 5). Additionally, it accounts for surface texture (frictional properties may change during fatigue due to sweating). Thus, safety margins computed using a soft-contact model provide insights into a complementary aspect of grasp planning and execution that reflect how participants account for the properties of the tissue and object at the contact.

Our main objective in this paper was to introduce safety margins using a soft-contact model. We used an experimental study (Singh, et al., 2013) involving fatigue as a

physiological perturbation to show that the complex changes in the applied slip vector (especially applied free moments) are more systematically captured by a soft-contact model rather than a hard-contact model. Dexterous tasks such as writing with a pen or grasping a wine glass, rely on application of free moments in a controlled fashion (Birznieks, et al., 2010). Therefore, incorporating and quantifying the role of free moments in grasp planning and execution would yield insights that are not possible with the widely used hard-contact model. The soft-contact model proposed in this paper provides a novel theoretical framework for the quantification of safety margins to address such problems. However, there are also technological challenges to studying grasping of objects with complex features. For example, how does one instrument a pen or a wine glass with force and motion transducers without substantially altering their inertial properties (though cf. Shim, et al., 2010)? Through the combination of our theoretical framework and innovative technological solutions to instrumenting real-world objects, novel questions in human prehension can be methodically addressed.

Acknowledgements

The authors thank Drs. Vladimir Zatsiorsky and Mark Latash for allowing us to reanalyze data from a previously published study (Singh, et al., 2014). The study was in part supported by NIH grants AG-018751, NS-035032, and AR-048563 awarded to Drs. Zatsiorsky and Latash.

5 References

Adams, M. J., Johnson, S. A., Lefèvre, P., Lévesque, V., Hayward, V., André, T., & Thonnard, J.-L. (2013). Finger pad friction and its role in grip and touch. *Journal of The Royal Society Interface, 10*.

Aoki, T., Niu, X., Latash, M. L., & Zatsiorsky, V. M. (2006). Effects of friction at the digit-object interface on the digit forces in multi-finger prehension. *Experimental Brain Research, 172*, 425-438.

Birznieks, I., Wheat, H. E., Redmond, S. J., Salo, L. M., Lovell, N. H., & Goodwin, A. W. (2010). Encoding of tangential torque in responses of tactile afferent fibres innervating the fingerpad of the monkey. *Journal of Physiology, 588*, 1057-1072.

Cadoret, G., & Smith, A. M. (1996). Friction, not texture, dictates grip forces used during object manipulation. *Journal of Neurophysiology, 75*, 1963-1969.

Carpentier, A., Duchateau, J., & Hainaut, K. (2001). Motor unit behaviour and contractile changes during fatigue in the human first dorsal interosseus. *Journal of Physiology, 534*, 903-912.

Cole, K. J., Rotella, D. L., & Harper, J. G. (1999). Mechanisms for age-related changes of fingertip forces during precision gripping and lifting in adults. *Journal of Neuroscience, 19*, 3238-3247.

Flanagan, J. R., & Johansson, R. S. (2010). Object representations used in action and perception. *Motor Control: Theories, Experiments, and Applications: Theories, Experiments, and Applications*, 30-49.

Hermsdörfer, J., Hagl, E., Nowak, D., & Marquardt, C. (2003). Grip force control during object manipulation in cerebral stroke. *Clinical Neurophysiology, 114*, 915-929.

Hertz, H. (1882). On the contact of rigid elastic solids on hardness. In. New York: Macmillan.

Jenmalm, P., Goodwin, A. W., & Johansson, R. S. (1998). Control of grasp stability when humans lift objects with different surface curvatures. *Journal of Neurophysiology, 79*, 1643-1652.

Johansson, R. S., & Westling, G. (1984). Roles of glabrous skin receptors and sensorimotor memory in automatic control of precision grip when lifting rougher or more slippery objects. *Experimental Brain Research, 56*, 550-564.

Kao, I., & Cutkosky, M. R. (1992). Quasistatic manipulation with compliance and sliding. *The International Journal of Robotics Research, 11*, 20-40.

Kinoshita, H., Bäckström, L., Flanagan, J. R., & Johansson, R. S. (1997). Tangential torque effects on the control of grip forces when holding objects with a precision grip. *Journal of Neurophysiology, 78*, 1619-1630.

Li, Y., & Kao, I. (2001). A review of modeling of soft-contact fingers and stiffness control for dextrous manipulation in robotics. In *IEEE International Conference on Robotics and Automation* (Vol. 3, pp. 3055- 3060).

Luu, B. L., Day, B. L., Cole, J. D., & Fitzpatrick, R. C. (2011). The fusimotor and reafferent origin of the sense of force and weight. *Journal of Physiology, 589*, 3135-3147.

Murray, R. M., Li, Z., & Sastry, S. S. (1994). *A mathematical introduction to robotic manipulation* (First ed.). Boca Raton, FL: CRC Press.

Nowak, D. A. (2008). The impact of stroke on the performance of grasping: usefulness of kinetic and kinematic motion analysis. *Neuroscience & Biobehavioral Reviews, 32*, 1439-1450.

Rost, K., Nowak, D. A., Timmann, D., & Hermsdörfer, J. (2005). Preserved and impaired aspects of predictive grip force control in cerebellar patients. *Clinical Neurophysiology, 116*, 1405-1414.

Savescu, A. V., Latash, M. L., & Zatsiorsky, V. M. (2008). A technique to determine friction at the finger tips. *Journal of Applied Biomechanics, 24*, 43-50.

Seo, N. J., Armstrong, T. J., & Drinkaus, P. (2009). A comparison of two methods of measuring static coefficient of friction at low normal forces: a pilot study. *Ergonomics, 52*, 121-135.

Shim, J. K., Hooke, A. W., Kim, Y.-S., Park, J., Karol, S., & Kim, Y. H. (2010). Handwriting: hand-pen contact force synergies in circle drawing tasks. *Journal of Biomechanics, 43*, 2249-2253.

Shim, J. K., Latash, M. L., & Zatsiorsky, V. M. (2005). Prehension synergies in three dimensions. *Journal of Neurophysiology, 93*, 766-776.

Singh, T., & Ambike, S. (2015). A soft-contact and wrench based approach to study grasp planning and execution. *Journal of Biomechanics, 48*, 3961–3967.

Singh, T., Zatsiorsky, V. M., & Latash, M. L. (2013). Adaptations to fatigue of a single digit violate the principle of superposition in a multi-finger static prehension task. *Experimental Brain Research, 225*, 589-602.

Singh, T., Zatsiorsky, V. M., & Latash, M. L. (2014). Prehension synergies during fatigue of a single digit: Adaptations in control with referent configurations. *Motor Control, 18*, 278-296.

Tomlinson, S. E., Lewis, R., & Carré, M. J. (2007). Review of the frictional properties of finger-object contact when gripping. *Proceedings of the Institution of Mechanical Engineers, Part J: Journal of Engineering Tribology, 221*, 841-850.

Westling, G., & Johansson, R. S. (1984). Factors influencing the force control during precision grip. *Experimental Brain Research, 53*, 277-284.

Xia, T., & Law, L. A. F. (2008). A theoretical approach for modeling peripheral muscle fatigue and recovery. *Journal of Biomechanics, 41*, 3046-3052.

Xydas, N., & Kao, I. (1999). Modeling of contact mechanics and friction limit surfaces for soft fingers in robotics, with experimental results. *The International Journal of Robotics Research, 18*, 941-950.

Yoshikawa, T. (2010). Multifingered robot hands: Control for grasping and manipulation. *Annual Reviews in Control, 34*, 199-208.

6 Figure Captions

Figure 1: Friction models. A) The hard-contact friction model; the applied slip vector ($\mathbf{W_{applied}}$= [F_X, F_Y, F_Z]) is constrained to lie within the boundaries of the friction limit surface (cone). B) The soft-contact model; the slip vector ($\mathbf{W_{applied}}$= [F_X, F_Y, T_Z]) shown in red is constrained to lie within the friction limit surface (ellipse). The volume encompassed by FLS is dictated by the applied normal force.

Figure 2: Safety margins (SM) predictions using simulations. SM_{Hard} (hard-contact) and SM_{Soft} (soft-contact) models as a function of normal force (panel A) and free moment (panel B). The gold circles indicate T_Z>0 (panel A) and F_Y>0 (panel B). Safety margins are lower in these conditions compared to when T_Z=0 and F_Y=0, respectively. In both panels, F_X=4 N. F_Y=0 N in panel A and F_Z=15 N in panel B.

Figure 3: Experimental setup. The instrumented handle with the force transducers and kinematic sensors. An adjustable external weight could be moved to different locations to apply pronation (PR), supination (SU) or no (NEUT) external torques. These external torques elicited strong tangential forces and free moments at the digits. The setup used for fatiguing the thumb is shown in the inset.

Figure 4: Group data for the wrench components of the fatigued digit, the thumb, and the soft-contact model. A) The magnitude of the normal force (F_Z) decreased but all other wrench components (F_X, F_Y and T_Z) increased during fatigue. ⋆⋆ indicates $p<0.01$ and ⋆⋆⋆ indicates $p<0.001$. B) During fatigue, the average magnitude of the horizontal

forces (F_X, F_Y) and moments (T_Z) increased resulting in an increased magnitude of the slip vector (blue arrow=before fatigue, green arrow=during fatigue). The lower magnitude of the normal force resulted in smaller FLS (mesh ellipse). Thus, the slip vector was closer to the boundary of the FLS during fatigue, resulting in a less stable grasp. C) Shows a 2D projection of the figure in panel B. Since the applied horizontal tangential forces were relatively small, the differences in the relative magnitudes of the two slip vectors can be seen more clearly in the XZ plane.

Figure 5: Safety margins (group results). Scatter plot of SM_{Hard} (panel A) and SM_{Soft} (panel B). The circles indicate individual subjects in all three torque conditions (PR, NEUT, and SU) and teal line indicates no changes between the before and during fatigue conditions. During fatigue, the drop in SM_{Hard} was larger than the change in SM_{Soft}.

Figure(s)

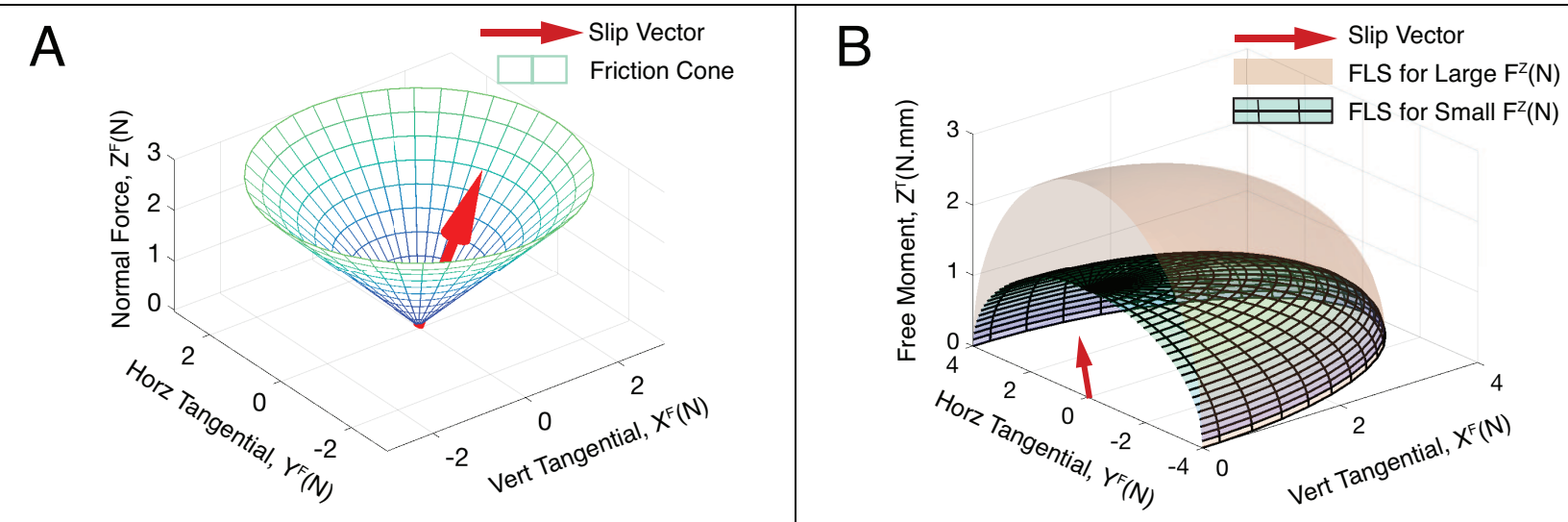
A
Slip Vector
Friction Cone
Normal Force, Z^F(N)
3
2
1
0
2
0
-2
Horz Tangential, Y^F(N)
-2
0
2
Vert Tangential, X^F(N)
B
Slip Vector
FLS for Large F^Z(N)
FLS for Small F^Z(N)
Free Moment, Z^T(N.mm)
3
2
1
0
4
2
0
-2
-4
Horz Tangential, Y^F(N)
0
2
4
Vert Tangential, X^F(N)

Figure(s)

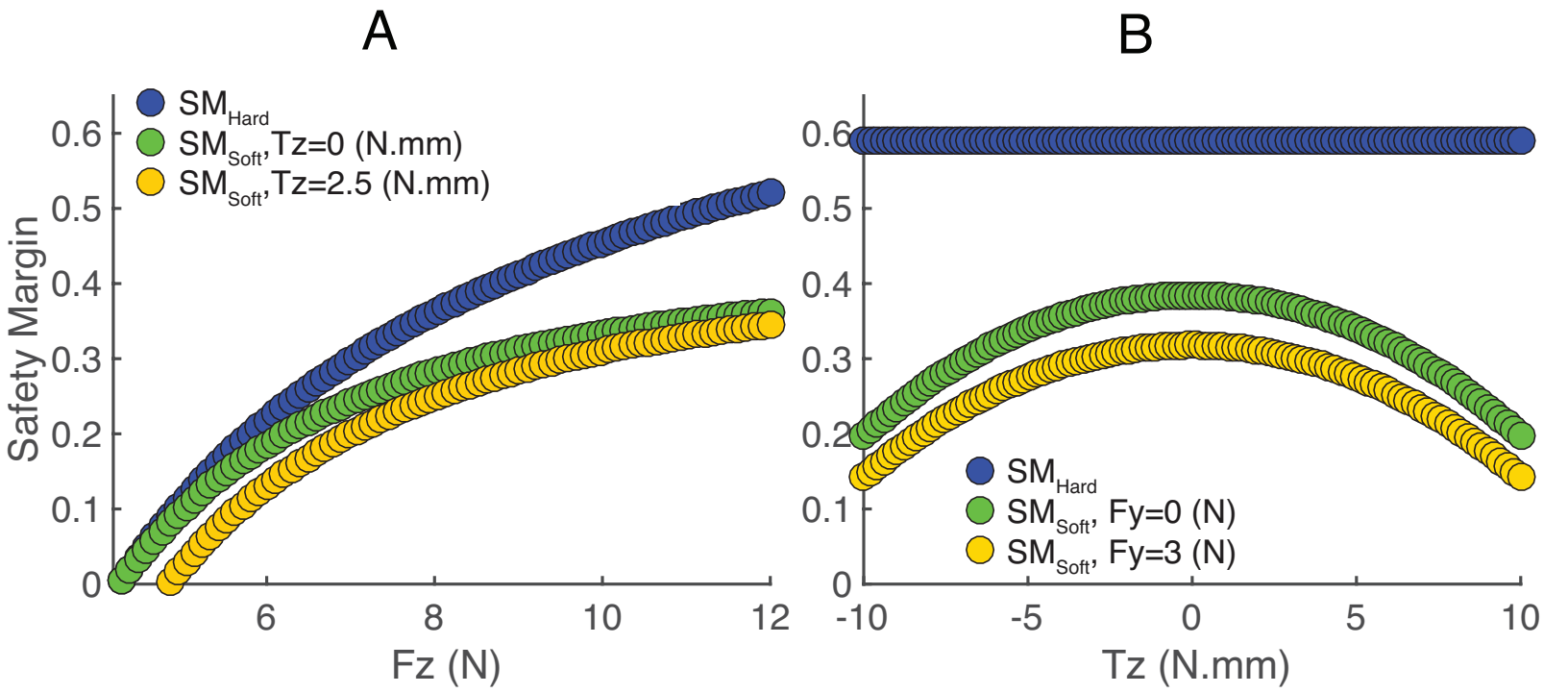
A
B
SM Hard
SM Soft, Tz=0 (N.mm)
SM Soft, Tz=2.5 (N.mm)
Safety Margin
0
0.1
0.2
0.3
0.4
0.5
0.6
6
8
10
12
Fz (N)
SM Hard
SM Soft, Fy=0 (N)
SM Soft, Fy=3 (N)
-10
-5
0
5
10
Tz (N.mm)

Figure(s)

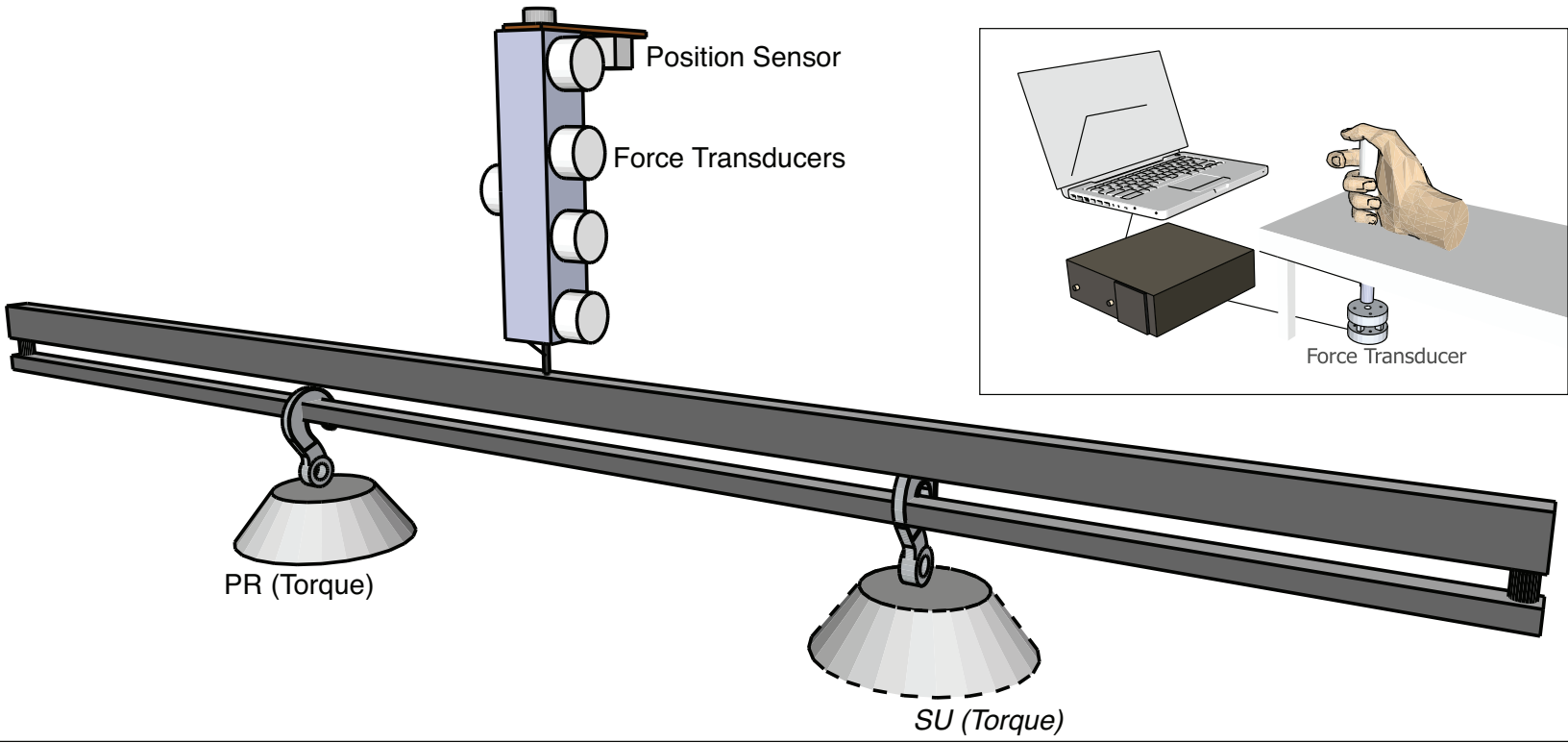
Position Sensor
Force Transducers
PR (Torque)
SU (Torque)
Force Transducer

Figure(s)

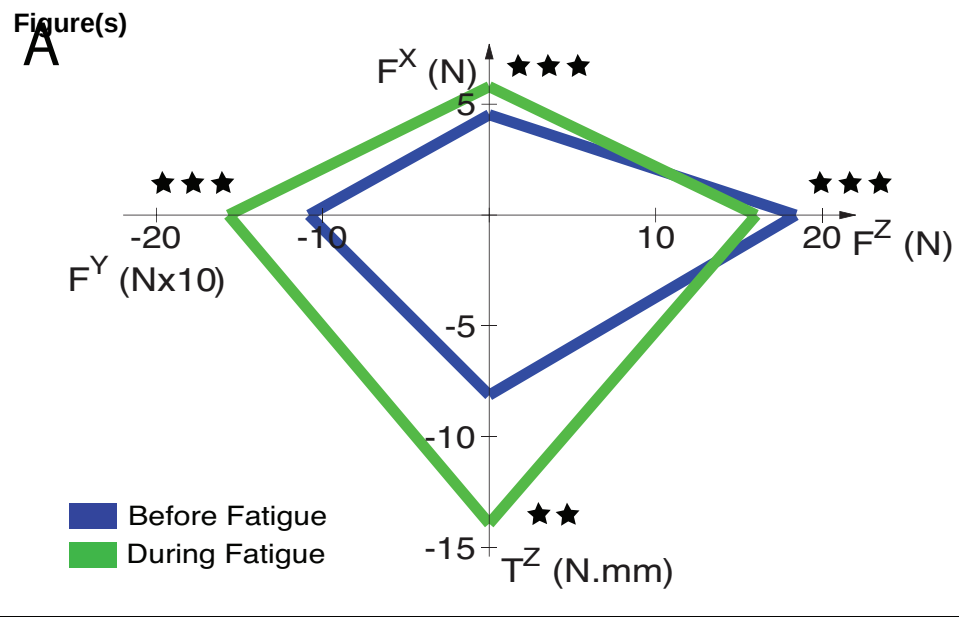
A
F^X (N)
5
-20
-10
10
20
F^Z (N)
F^Y (Nx10)
-5
-10
-15
T^Z (N.mm)
Before Fatigue
During Fatigue

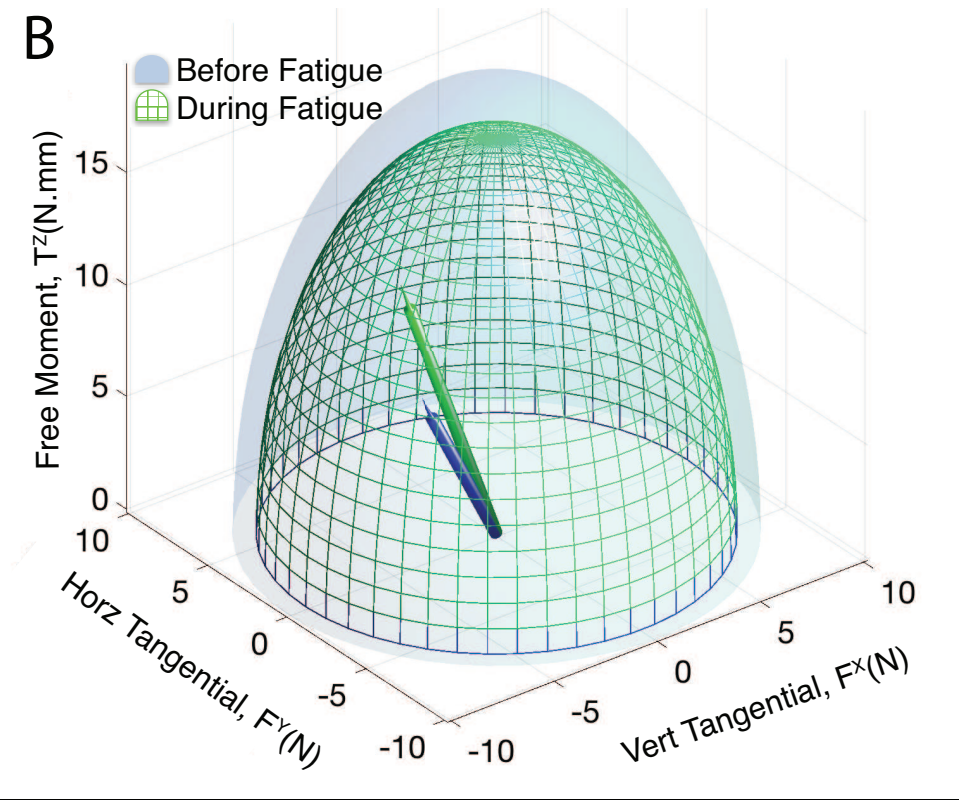
B
Before Fatigue
During Fatigue
Free Moment, T^Z(N.mm)
15
10
5
0
10
5
0
-5
-10
Horz Tangential, F^Y(N)
-10
-5
0
5
10
Vert Tangential, F^X(N)

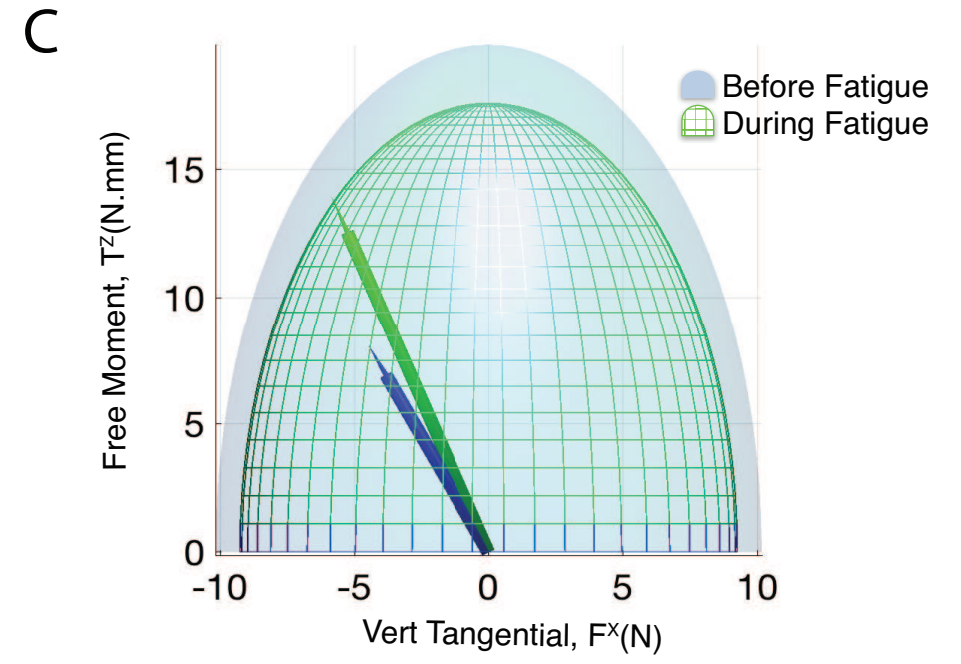
C
Before Fatigue
During Fatigue
Free Moment, T^Z(N.mm)
15
10
5
0
-10
-5
0
5
10
Vert Tangential, F^X(N)

Figure(s)

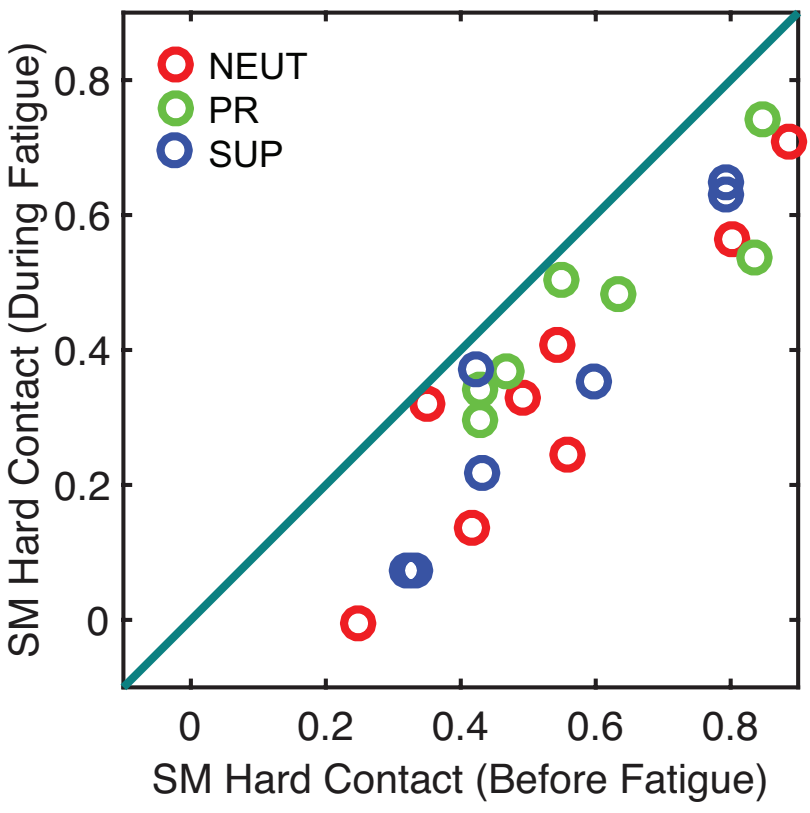
NEUT
PR
SUP
SM Hard Contact (During Fatigue)
SM Hard Contact (Before Fatigue)
0
0.2
0.4
0.6
0.8

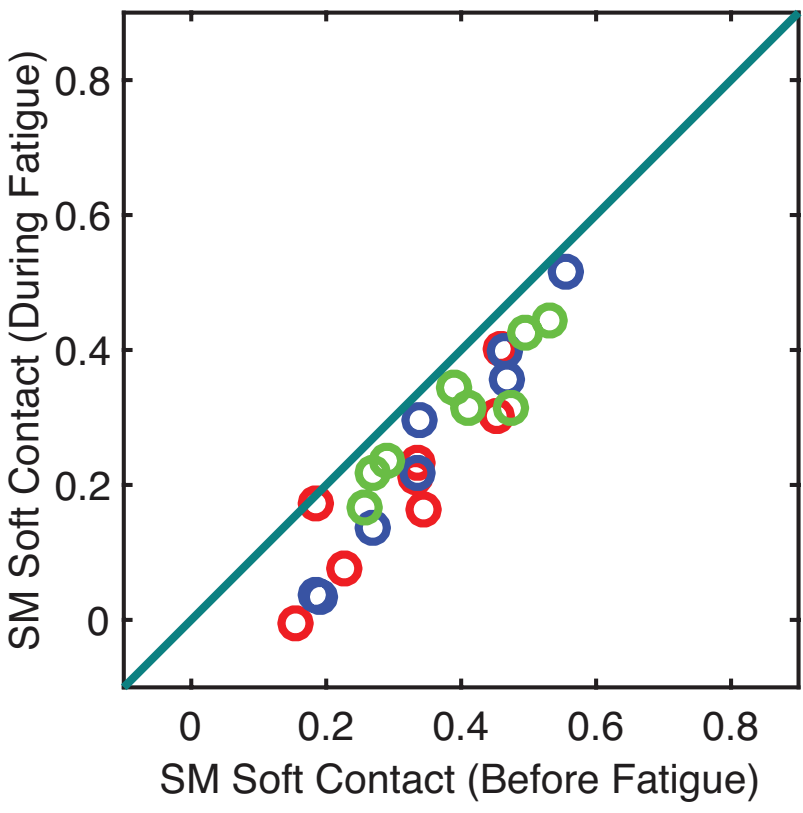
SM Soft Contact (During Fatigue)
SM Soft Contact (Before Fatigue)
0
0.2
0.4
0.6
0.8